

NATIONAL ADVISORY COMMITTEE FOR AERONAUTICS

# WARTIME REPORT

ORIGINALLY ISSUED

February 1945 as  
Advance Confidential Report L5A13

DETERMINATION OF THE STABILITY AND CONTROL CHARACTERISTICS  
OF A TAILLESS ALL-WING AIRPLANE MODEL WITH SWEEPBACK  
IN THE LANGLEY FREE-FLIGHT TUNNEL

By John P. Campbell and Charles L. Seacord, Jr.

Langley Memorial Aeronautical Laboratory  
Langley Field, Va.

233

FILE COPY  
To be retained  
RECEIVED BY R.C.S.  
of the  
OCT 7 1946  
for Aeronautics  
WASHINGTON

# NACA

WASHINGTON

NACA WARTIME REPORTS are reprints of papers originally issued to provide rapid distribution of advance research results to an authorized group requiring them for the war effort. They were previously held under a security status but are now unclassified. Some of these reports were not technically edited. All have been reproduced without change in order to expedite general distribution.

931 1100A-1000

NATIONAL ADVISORY COMMITTEE FOR AERONAUTICS

ADVANCE CONFIDENTIAL REPORT

DETERMINATION OF THE STABILITY AND CONTROL CHARACTERISTICS  
OF A TAILLESS ALL-WING AIRPLANE MODEL WITH SWEEPBACK  
IN THE LANGLEY FREE-FLIGHT TUNNEL

By John P. Campbell and Charles L. Seacord, Jr.

SUMMARY

An investigation to determine the power-off stability and control characteristics of a tailless all-wing airplane model with sweepback has been made in the Langley free-flight tunnel. The results of the free-flight-tunnel tests were correlated with results from force tests made at high Reynolds numbers in order to estimate the flying characteristics of the full-scale airplane.

The investigation consisted of force and flight tests of a 4.3-foot-span dynamic model. The effects of flap deflection, center-of-gravity location, and addition of vertical-tail area were determined.

The following conclusions were drawn from the results of the investigation: The full-scale airplane will undergo a serious reduction in stick-fixed longitudinal stability at high lift coefficients unless early wing-tip stalling is eliminated. The directional stability of an all-wing airplane without vertical tail surfaces will be undesirably low. The effective dihedral of an airplane of this type should be kept low. An elevon and rudder control system similar to that used on this design should provide sufficient control.

INTRODUCTION

The desire to obtain improved performance for military airplanes has recently increased the interest in tailless-airplane designs. One of the most promising tailless designs, from the considerations of performance,

is the large all-wing airplane or "flying wing." Inherent in the all-wing airplane, however, are certain undesirable stability and control characteristics that must be eliminated before this design can be considered satisfactory. In order to study these stability and control characteristics and to find means of improving them, an investigation is being conducted in the Langley free-flight tunnel (designated FFT) of a free-flying dynamic model of a tailless all-wing airplane with sweepback.

The present report gives the results of force and flight tests of the model with windmilling propellers. Tests were made with the lift flaps retracted and deflected. For some tests, auxiliary vertical tail surfaces were installed on the model. The effects of changes in the center-of-gravity location and trim lift coefficient on the flight characteristics of the model were determined.

In order to estimate the flying characteristics of the full-scale airplane, the test results were correlated with results of force tests of a similar design run at high Reynolds numbers in the Langley 19-foot pressure tunnel (designated 19-ft PT).

### SYMBOLS

The following symbols are used herein:

$C_L$	lift coefficient ( $Lift/qS$ )
$C_D$	drag coefficient ( $Drag/qS$ )
$C_m$	pitching-moment coefficient ( $Pitching\ moment/q\bar{c}S$ )
$C_l$	rolling-moment coefficient ( $Rolling\ moment/qbS$ )
$C_n$	yawing-moment coefficient ( $Yawing\ moment/qbS$ )
$C_Y$	lateral-force coefficient ( $Lateral\ force/qS$ )
$c$	chord, feet
$\bar{c}$	mean aerodynamic chord, feet

- S wing area, square feet
- b wing span, feet
- q dynamic pressure, pounds per square foot  $\left(\frac{1}{2}\rho V^2\right)$
- V airspeed, feet per second
- $\rho$  mass density of air, slugs per cubic foot
- $\beta$  angle of sideslip, degrees
- $\psi$  angle of yaw, degrees (for force-test data,  
 $\psi = -\beta$ )
- $\alpha$  angle of attack, degrees
- h static margin, distance in chords from center of gravity to neutral point
- $\frac{pb}{2V}$  helix angle generated by wing tip in roll, radians
- p rolling angular velocity, radians per second
- $C_{l_p}$  rate of change of rolling-moment coefficient with  
helix angle  $\left[\frac{\partial C_l}{\partial \left(\frac{pb}{2V}\right)}\right]$
- $C_{n_\beta}$  rate of change of yawing-moment coefficient with  
angle of sideslip, per degree  $(\partial C_n / \partial \beta)$
- $C_{l_\beta}$  rate of change of rolling-moment coefficient with  
angle of sideslip, per degree  $(\partial C_l / \partial \beta)$
- $\delta_f$  flap deflection, degrees
- $\delta_e$  elevon deflection, positive down, degrees (with  
subscripts r and l to indicate right and  
left elevon, respectively)
- $\delta_r$  rudder deflection, positive down, degrees (with  
subscripts r and l to indicate right and  
left rudder, respectively; if both right and  
left top rudder surfaces are deflected  
simultaneously as longitudinal trim flaps, no  
subscript is used)

R Reynolds number

### APPARATUS

The investigation was made in the Langley free-flight tunnel, which is described in reference 1. A photograph of the test section of the tunnel showing the model in flight is presented in figure 1. Force tests to determine the static stability characteristics were made in the Langley free-flight tunnel with the model mounted on the six-component balance, which is described in reference 2.

The mass and dimensional characteristics of the model are as follows:

Weight, pounds . . . . .	2.55
Wing area, square feet . . . . .	2.51
Span, feet . . . . .	4.3
Aspect ratio . . . . .	7.36
Wing loading, pounds per square foot . . . . .	1.02
Radius of gyration in roll, $k_x$ , foot . . . . .	0.78
Radius of gyration in pitch, $k_y$ , foot . . . . .	0.35
Radius of gyration in yaw, $k_z$ , foot . . . . .	0.82
Mean aerodynamic chord, foot . . . . .	0.655
Sweepback of 0.25-chord line, degrees . . . . .	22.00
Dihedral, degrees . . . . .	0
Taper ratio (ratio of tip chord to root chord) . . . . .	0.25
Root chord, foot . . . . .	0.937
Tip chord, foot . . . . .	0.234
Elevon:	
Type . . . . .	Plain
Area, percent wing area . . . . .	5.40
Span, percent wing span . . . . .	38.00
Rudder:	
Type . . . . .	Split, drag
Area, percent wing area . . . . .	2.86
Span, percent wing span . . . . .	20.00
Vertical tails:	
Type . . . . .	Twin center fins
Area, percent wing area . . . . .	4.00
Aspect ratio . . . . .	2.00

Airfoil section . . . . . Modified NACA 103  
Root, percent thickness . . . . . 21  
Tip, percent thickness . . . . . 15  
Geometric twist, degrees . . . . . 6  
Aerodynamic twist, degrees . . . . . (approx.) 4

The component parts of the model are identified in the tables and figures as follows:


Wing . . . . . W  
Propeller shaft housings . . . . . H  
Propellers . . . . . P  
Vertical tails; two tails mounted on nacelles,  
each tail having 2 percent of wing area . . . . . V  
Split flap (center-section lift flap,  $\delta_f = 60^\circ$ ) . . . F

Combinations of these letters represent the combination used in the tests. The standard configuration is designated WHP. A three-view drawing of the model is presented in figure 2. Photographs are given in figures 3 and 4. In plan form the wing has both sweepback and taper and has a split flap that extends from the center line of the airplane to the inboard ends of the elevons. For all flap-down tests, the flaps were deflected  $60^\circ$ .

The control surfaces consist of elevons that extend from  $0.33\frac{b}{2}$  to  $0.71\frac{b}{2}$  and split rudders (fig. 5) that extend from  $0.71\frac{b}{2}$  to  $0.91\frac{b}{2}$ . The split rudder is so linked with the elevon that in flight tests the lower surface of the rudder moves down with the downgoing elevon and the upper surface moves up with the upgoing elevon. This linkage arrangement provides additional effective aileron- and elevator-control-surface area as shown in figure 6.

The upper surfaces of the split rudders can be deflected upward simultaneously to serve as trim flaps to provide pitching moment for longitudinal trim when the lift flap is deflected. The lower surfaces of the split rudders remain at zero when the top surfaces are deflected as trim flaps.

The controls of the model were operated in flight by electromagnets in the same manner as described in reference 1.



For some tests vertical tail surfaces having a combined area of 4 percent of the wing area were mounted on the propeller-shaft housings to provide additional directional stability. (See figs. 2 and 4.)


For propeller-on tests the model was equipped with two freely windmilling two-blade pusher propellers.

A modified NACA 103 airfoil with a thickness of 21 percent at the root and 15 percent at the tip was used on the model. The trailing edge was reflexed enough to give a slightly positive pitching moment at zero lift. This airfoil was used to obtain a maximum lift coefficient in the free-flight (low Reynolds number) tests more nearly equal to that of a full-scale airplane than is possible to obtain with other airfoils (especially low-drag airfoils) at low Reynolds numbers.

The free-flight-tunnel model was almost identical in plan form to the model used in the tests at higher Reynolds numbers in the Langley 19-foot pressure tunnel. The models differed in airfoil section, geometric dihedral, and geometric twist. The airfoil sections of the model tested in the Langley 19-foot pressure tunnel were NACA 65(318)-019 at the root and 65(318)-015 at the tip; the geometric dihedral of this model was  $2^\circ$  compared with  $0^\circ$  for the free-flight-tunnel model. The model used in the Langley 19-foot pressure tunnel had  $4^\circ$  geometric twist, whereas the free-flight-tunnel model had a geometric twist of  $6^\circ$ . The aerodynamic twist for both models, however, was approximately  $4^\circ$ .

## TESTS

Force tests were made to determine the stability and control characteristics of the model with flaps retracted and deflected. The moments were computed with the center of gravity at 0.25 mean aerodynamic chord and are referred to the stability axes. The stability axes are defined as an orthogonal system of axes in which the Z-axis is in the plane of symmetry and perpendicular to the relative wind, the X-axis is in the plane of symmetry and perpendicular to the Z-axis, and the Y-axis is perpendicular to the plane of symmetry. The conditions in which force tests were made are given in table I.





Flight tests were made at lift coefficients varying from 0.3 to 0.8 with flaps retracted and from 0.6 to 1.1 with flaps deflected. The center-of-gravity position was varied from 20 to 25 percent of the mean aerodynamic chord for flight tests in both the flap-retracted and flap-deflected condition. Table II gives the conditions for which flight tests were made.

## RESULTS AND DISCUSSION

In interpreting the results of the free-flight-tunnel tests of the tailless all-wing model the following points were considered:

(1) The tests were made at very low Reynolds numbers (150,000 to 350,000); hence, the results of the tests of a similar design made at high Reynolds numbers (about 6,600,000) were used in estimating the flight characteristics of the full-scale airplane from the free-flight-tunnel test results.

(2) The controls of the model were fixed except during control applications; hence, no indications of the control-free stability of the design were obtained.


(3) In determining the control effectiveness of the design, no consideration has been given to control forces.

(4) No power was applied to the propellers during the tests. The results, therefore, cannot be used to predict power-on stability.

### Longitudinal Stability

Force tests.— The results of force tests made to determine the longitudinal stability and control characteristics of the model are shown in figures 7 and 8. On these figures, data from tests of the model of similar plan form tested at high Reynolds numbers are also plotted.

The slope of the pitching-moment curve for the flap-retracted condition of the free-flight-tunnel model changes from negative to positive with increasing lift coefficient. This change in slope indicates a change to



static longitudinal instability at high angles of attack. This change in stability is characteristic of swept-back wings because of the tendency of the wing tips to stall first. The instability appears to be much greater for the free-flight-tunnel model than for the similar model tested at high Reynolds numbers. This difference is probably explained by the fact that the difference in the Reynolds numbers at the root and tip sections of this design causes a much greater difference in stalling characteristics on the small-scale model than on the model tested at high Reynolds numbers.

For the flap-deflected condition (fig. 8), the pitching-moment curves for the free-flight-tunnel model were very similar in shape to those obtained with flaps up but did not turn up at high lift coefficients as much as the curves for the flap-retracted condition. The data of figure 8 indicate that most of the change in shape of the pitching-moment curve from flap up to flap down was caused by the upward deflection of the trim flap. The flap-deflected pitching-moment curve from high-scale tests (fig. 8) indicates practically no change in longitudinal stability with increasing angle of attack.

The difference in the angles of zero lift indicated in figures 7 and 8 for the two models is probably caused by the difference in the location of the chord line from which the angle of attack is measured. The difference in the slopes of the lift curve is probably a result of the difference in the Reynolds numbers of the tests. It is unlikely that these differences in lift characteristics would cause appreciable differences in longitudinal flight characteristics.

Flight tests.- The longitudinal stability as noted in the free-flight-tunnel tests was satisfactory up to a lift coefficient of 0.7 with flaps retracted and 1.1 with flaps deflected with the normal center-of-gravity location (25 percent M.A.C.). Above these values of lift coefficient, however, difficulty was experienced in flying the model because of a tendency to nose up and stall after disturbances in pitch. This behavior was believed to be a direct result of the change in longitudinal stability at high angles of attack, which was indicated in the force-test results by the change in slope of the pitching-moment curve. Although at times the pilot could prevent the nosing-up motion by applying down-elevator control,

CONFIDENTIAL


the nosing-up tendency was considered a very objectionable characteristic that would probably prove dangerous for a full-scale airplane. This nosing-up tendency should be expected on any airplane having pitching-moment characteristics similar to those of the model. (See fig. 7.)

The longitudinal stability of the free-flight-tunnel model was satisfactory at those lift coefficients at which the static margin  $h$  was 0.04 or greater ( $C_L = 0.7$ , flaps retracted;  $C_L = 1.1$ , flaps deflected) and flights were possible at conditions at which the static margin was as low as 0.02. On the basis of the force-test results it appears that the static longitudinal stability of the corresponding airplane at high angles of attack would be greater than that of the free-flight-tunnel model. The data of figures 7 and 8 indicate that the airplane with the normal center-of-gravity location would have a static margin of 0.04 up to a lift coefficient of 1.0 with flaps retracted and up to the stall with flaps deflected. The stick-fixed longitudinal stability of this particular airplane design, therefore, would probably be satisfactory for all power-off conditions except at high lift coefficients with flaps retracted.

### Longitudinal Control

The force-test results presented in figures 7 and 8 indicate that the longitudinal control provided by the elevons was sufficient to trim the model over the flight range for flap-retracted or-deflected condition with a total elevon deflection of about  $20^\circ$ . Inasmuch as the force-test results of the model tested at high Reynolds numbers indicate much more powerful elevon control than was obtained with the model at low Reynolds numbers, it is probable that the elevator control for the full-scale airplane will be satisfactory in flight.

In the flight tests, the model could be trimmed over the speed range with a total elevon deflection of about  $20^\circ$ . For the flap-retracted condition, the upper surfaces of the split rudders were deflected with the elevons for longitudinal trim. Abrupt elevon deflections of  $\pm 5^\circ$  from the trim setting provided adequate longitudinal control for keeping the model flying for all stable conditions.



On this design it is possible that the most critical condition for elevator control will be at take-off. Unless careful attention is given to the location of the landing gear, the elevons alone may not be powerful enough to meet the Army requirements for getting the nose wheel off the ground at 80 percent of take-off speed. Use of the trim flaps in conjunction with the elevons will help provide enough longitudinal control to meet this requirement.

### Lateral Stability

Force tests.- The lateral stability characteristics of the model as determined by force tests are shown in figures 9 to 11. The values of the effective-dihedral parameter  $C_{l\beta}$  and the directional-stability parameter  $C_{n\beta}$  obtained for the different test conditions from these figures are plotted in figure 12 in the form of a stability diagram. The values of  $C_{n\beta}$  and  $C_{l\beta}$  for corresponding conditions for the model tested at high Reynolds numbers are also presented in figure 12.

The values of  $C_{n\beta}$  for the flap-retracted condition at angles of attack of  $0^\circ$  and  $6^\circ$  are relatively low (about 0.00030). Increasing the angle of attack to  $12^\circ$  with flaps retracted caused an increase in  $C_{n\beta}$  to 0.00055. This increase in  $C_{n\beta}$  with increase in lift coefficient is characteristic of a swept-back wing.

The lower values of  $C_{n\beta}$  shown in figure 12 for the model tested at high Reynolds numbers are attributed to the lower drag of this model. For an all-wing tailless design with low dihedral, the drag of the wing contributes a major part of the static directional stability.

The values of  $C_{l\beta}$  shown for the free-flight model in figure 12 correspond to an effective dihedral angle between  $2^\circ$  and  $4^\circ$ . The value of  $C_{l\beta}$  increased with increasing lift coefficient as expected for the swept-back wing. The higher values of  $C_{l\beta}$  for the model tested at large Reynolds numbers is caused by the fact

that this model had 20° geometric dihedral whereas the free-flight-tunnel model had 0° geometric dihedral.

Flight tests.— The lateral stability characteristics of the model noted in flight were fairly satisfactory except for low directional stability in the flap-retracted condition. This low directional stability was shown principally by slow lightly damped yawing oscillations that were started by gust or control disturbances. The directional stability was not dangerously low, however, inasmuch as neither divergences nor unstable oscillations were noted. The adverse yawing noted in flights in which aileron control alone was used was quite small because the elevons were deflected upward together for longitudinal trim and therefore operated as "trimmed-up" ailerons, which usually produce only small yawing moments.

Deflection of the flaps or addition of the vertical tails caused noticeable improvement in the damping of the yawing motion of the model, and the lateral stability characteristics at these conditions were considered generally satisfactory.

The effective dihedral of the model appeared to be satisfactory, inasmuch as no excessive rolling during sideslip was noted and the lightly damped yawing oscillations were accompanied by very little rolling. Previous free-flight-tunnel investigations have shown that, for an airplane with low directional stability, low effective dihedral is necessary to avoid a poorly damped rolling (Dutch roll) oscillation.

It is probable that the lateral stability characteristics of a full-scale airplane of the design tested would not be so good as those of the free-flight model because the values of  $C_{n\beta}$  of a full-scale airplane will probably be lower than those for the free-flight model. At the higher lift coefficients, which could not be reached in the free-flight-tunnel tests because of longitudinal instability, the requirements of the airplane would be more severe for directional stability and the airplane would probably be considered unsatisfactory in this respect. In order to secure satisfactory flying characteristics with a tailless all-wing airplane of this type, it appears desirable to maintain a low value of effective dihedral and to supplement the directional stability of the wing by means of vertical tails or an automatic stabilizing device.

## Lateral Control

Aileron control.- The aileron control provided by the elevons appeared to be weak in the flight tests. Abrupt elevon deflections of  $\pm 15^\circ$  did not provide satisfactory aileron control in flight. Previous free-flight-tunnel tests have shown that, if aileron deflections greater than  $\pm 15^\circ$  are required for satisfactory control on a model, the ailerons on the corresponding airplane are likely to be weak.

A better quantitative indication of the weakness of the aileron control was obtained in the force tests, the results of which are presented in figures 13 and 14 and which are summarized and compared in figure 15 with results of tests at high Reynolds numbers. Computed values of the helix angle  $pb/2V$  produced at different lift coefficients by various elevon deflections are shown in figure 15. The values of  $pb/2V$  were obtained by multiplying the force-test values of rolling-moment coefficient by  $0.8/C_{l_p}$ . (See reference 3.) The high Reynolds number data of figure 15 indicate that the flying-qualities requirement for a minimum value of 0.07 for  $pb/2V$  is not met by this design at lift coefficients above about 0.4 with  $\pm 15^\circ$  elevon deflection. The free-flight-tunnel force tests indicate even weaker aileron control but this result is partly attributed to the low Reynolds number of the tests, to the wing section used, and to the initial reflex of the trailing edge of the wing. The free-flight-tunnel test results do indicate, however, that linking the rudder surfaces to move as ailerons with the elevons provides a substantial improvement in aileron control.

In order to obtain satisfactory aileron control with elevon surfaces located well inboard of the tip as on this design, larger-chord surfaces than those on the free-flight-tunnel model should be used or the rudder surfaces should be linked with the elevons in order to provide greater effective elevon area.

Rudder control.- The split rudders on the model provided sufficient yawing moments to balance out the adverse yawing moments encountered in the flight tests during aileron rolls. Inasmuch as the yawing moments caused by aileron deflection were small (fig. 14) because of the initial upward deflection of the elevons for

longitudinal trim; the rudder yawing moments only had to oppose the adverse yawing moments caused by rolling. The adverse yawing moments caused by rolling were apparently small for the model, as indicated by the small amount of adverse yawing in flights with rudders fixed and elevons alone used for control. These results indicate that the rudder control of this all-wing airplane should be adequate during normal flight.

Usually the most severe requirement for rudder control of multiengine airplanes is that the rudder control balance the asymmetric yawing moments introduced by the failure of one engine during a full-power climb. Calculations based on the force-test data presented in figure 16 indicate that, with rudders of the size and type used on this design, an airplane of this type having a 150-foot span and two 3000-horsepower engines would meet the Army requirements for maintaining steady flight with  $10^\circ$  or less sideslip at 120 percent of the stalling speed with one engine inoperative and the other engine operating at full power.

### CONCLUSIONS

The following conclusions concerning the power-off stability and control characteristics of large all-wing tailless airplanes with sweepback were drawn from the Langley free-flight-tunnel test results and from a correlation of these results with results obtained from force tests made at high Reynolds numbers:

1. Stick-fixed longitudinal instability at high lift coefficients, or at least a serious reduction in longitudinal stability, should be expected for airplanes of this type unless the premature stalling of the wing tips is eliminated. The upward deflection of a trim flap at the wing tip will reduce the tendency of the tips to stall first and will thereby improve the longitudinal stability at high lift coefficients.

2. The directional stability of this type of airplane without vertical tail surfaces will be extremely low. Although the airplane will be flyable, it will probably not be considered entirely satisfactory because of the tendency to sideslip to large angles following slight gust or control disturbances.

3. The effective dihedral of an airplane of this type should be kept low in order to minimize the amount of rolling accompanying the lightly damped yawing oscillations that are likely to be encountered.

4. An elevon and rudder control system similar to that used on the model in these tests should provide sufficient longitudinal and lateral control for an airplane of this type.

Langley Memorial Aeronautical Laboratory  
National Advisory Committee for Aeronautics  
Langley Field, Va.

#### REFERENCES

1. Shortal, Joseph A., and Osterhout, Clayton J.: Preliminary Stability and Control Tests in the NACA Free-Flight Wind Tunnel and Correlation with Full-Scale Flight Tests. NACA TN No. 810, 1941.
2. Shortal, Joseph A., and Draper, John W.: Free-Flight-Tunnel Investigation of the Effect of the Fuselage Length and the Aspect Ratio and Size of the Vertical Tail on Lateral Stability and Control. NACA ARR No. 3D17, 1943.
3. Kayten, Gerald G.: Analysis of Wind-Tunnel Stability and Control Tests in Terms of Flying Qualities of Full-Scale Airplanes. NACA ACR No. 3J22, 1943.



TABLE I

FORCE-TEST CONDITIONS FOR TAILLESS ALL-WING AIRPLANE MODEL  
IN THE LANGLEY FREE-FLIGHT TUNNEL

Test	$\alpha$ (deg)	$\psi$ (deg)	Configu- ration (a)	$\delta_e$ (deg)	$\delta_{r_l}$ (deg)	$\delta_{r_r}$ (deg)	Figure
1	-4 to 20	0	WHP	0	0	0	7
2	-4 to 20	0	WHPF	0	0	0	8
3	-4 to 16	0	WHP	-10	-10	-10	7
4	-4 to 16	0	WHPF	0	-40	-40	8
5	-4 to 16	0	WHPF	-10	-40	-40	8
6	0	-30 to 30	WHP	0	0	0	9
7	6	-30 to 30	WHP	-10	0	0	9
8	12	-30 to 30	WHP	-20	0	0	9
9	8	-30 to 30	WHPF	-10	-40	-40	10
10	6	-30 to 30	WHPV	-10	0	0	11
11	6	-30 to 30	W	-10	0	0	11
12	0 to 12	0	WHP	-10 (Right only)	0	0	13
13	0 to 12	0	WHP	10 (Right only)	0	0	13
14	0 to 12	0	WHP	-20 (Right only)	0	0	13
15	0 to 12	0	WHP	20 (Right only)	0	0	13
16	0 to 12	0	WHP	0	0	10	14
17	0 to 12	0	WHP	0	0	-10	14
18	0 to 12	0	WHP	0	0	-20	14
19	0 to 12	0	WHP	0	0	20	14
20	0 to 12	0	WHP	0	0	$\pm 20$	16
21	0 to 12	0	WHP	0	0	$\pm 40$	16
22	0 to 12	0	WHP	0	0	$\pm 60$	16

<sup>a</sup>Explanation of configurations is given in section on  
"Apparatus."

NATIONAL ADVISORY  
COMMITTEE FOR AERONAUTICS

03/12/2010 10:30

TABLE II  
FLIGHT-TEST CONDITIONS OF TAILLESS ALL-WING AIRPLANE  
MODEL IN LANGLEY FREE-FLIGHT TUNNEL

Lift coefficient	Configuration (a)	Center-of-gravity location (percent M.A.C.)
0.3 to 0.8	WHP	0.25
.6	WHPV	.25
.6	WHPV	.22
.5	WHPV	.20
.6 to 1.1	WHPVF	.25
.6 to 1.1	WHPF	.25
.7	WHPVF	.22
.7	WHPVF	.20

<sup>a</sup>Explanation of configurations given in section on  
"Apparatus."

NATIONAL ADVISORY  
COMMITTEE FOR AERONAUTICS

03:41:24.1030

DECLASSIFIED



Figure 1.- Test section of Langley free-flight tunnel showing model in flight.

CONFIDENTIAL

03742301030

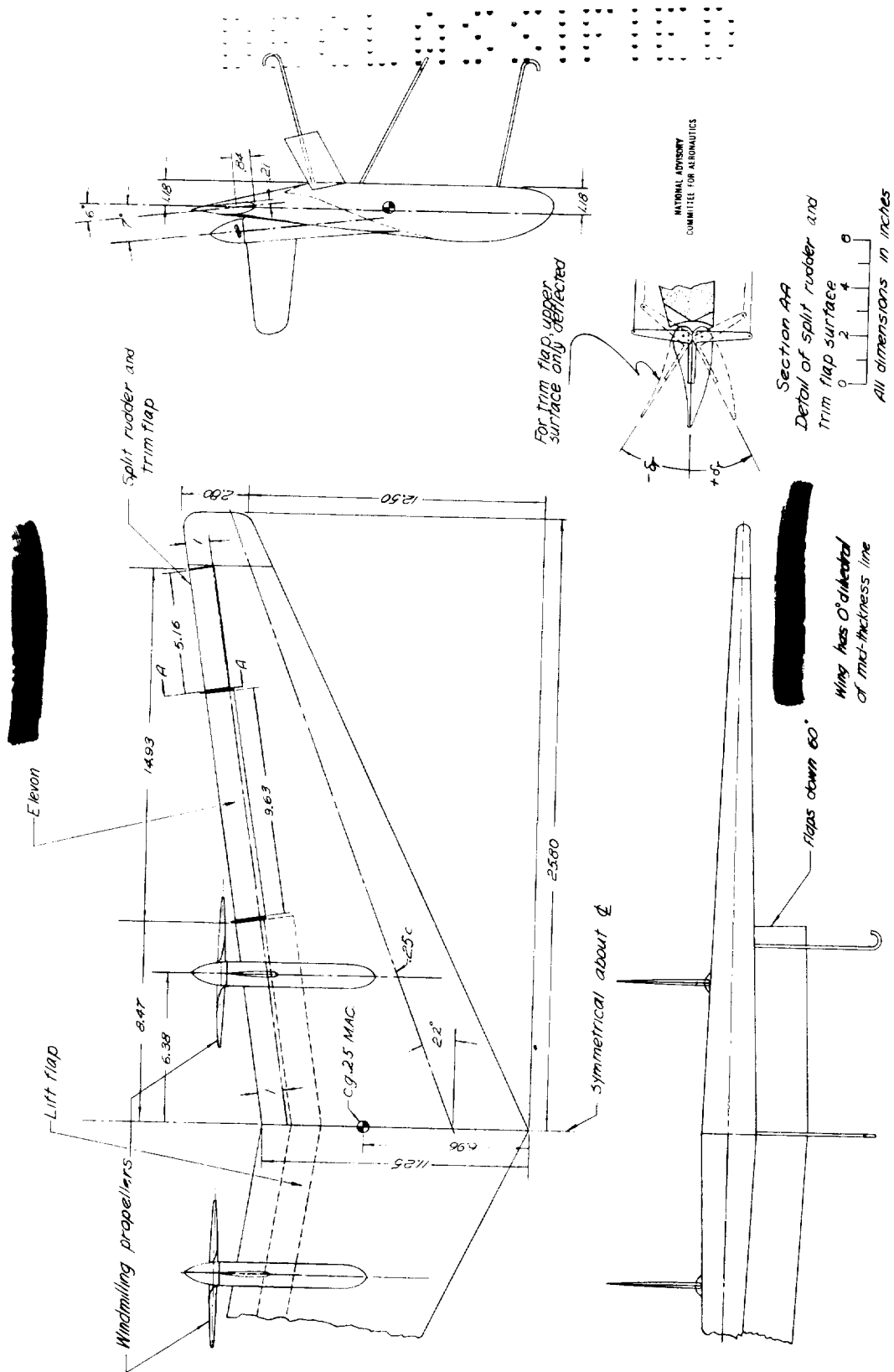


Figure 2.-Drawing of a tailless airplane model tested in the Langley free-flight tunnel.

03712301030



REPRODUCED

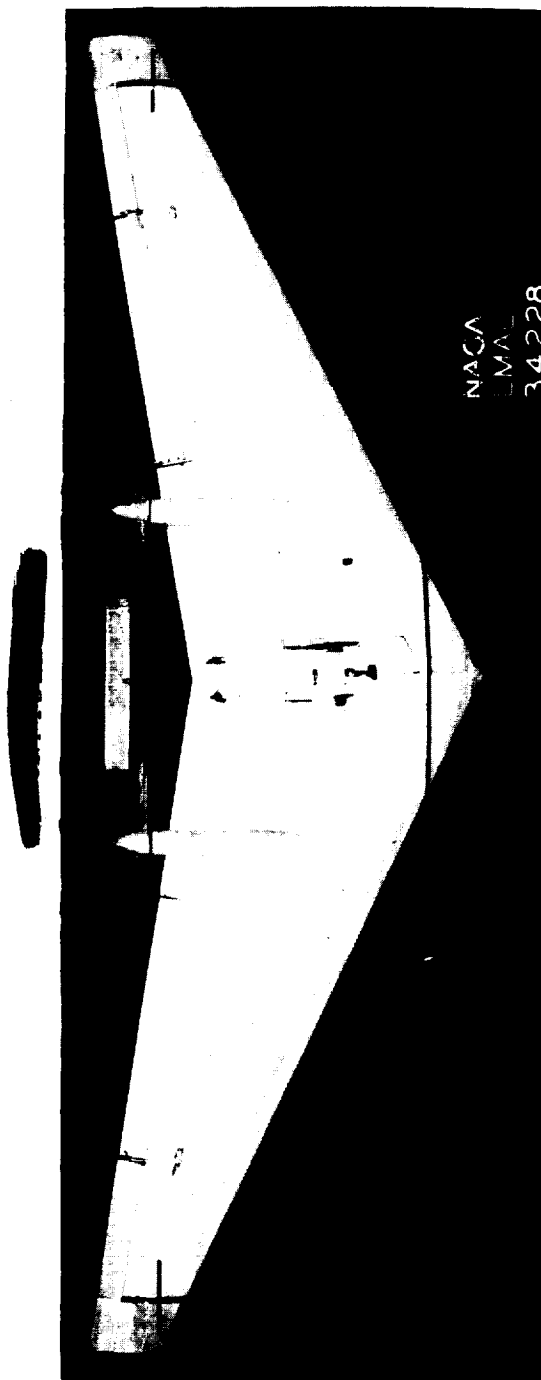


Figure 3.- Plan view of tailless all-wing model tested in Langley free-flight tunnel.

037123A.034



Figure 4.- Three-quarter front view of tailless all-wing model tested in Langley free-flight tunnel. Auxiliary vertical tails mounted on nacelles.

CONFIDENTIAL

03710201030

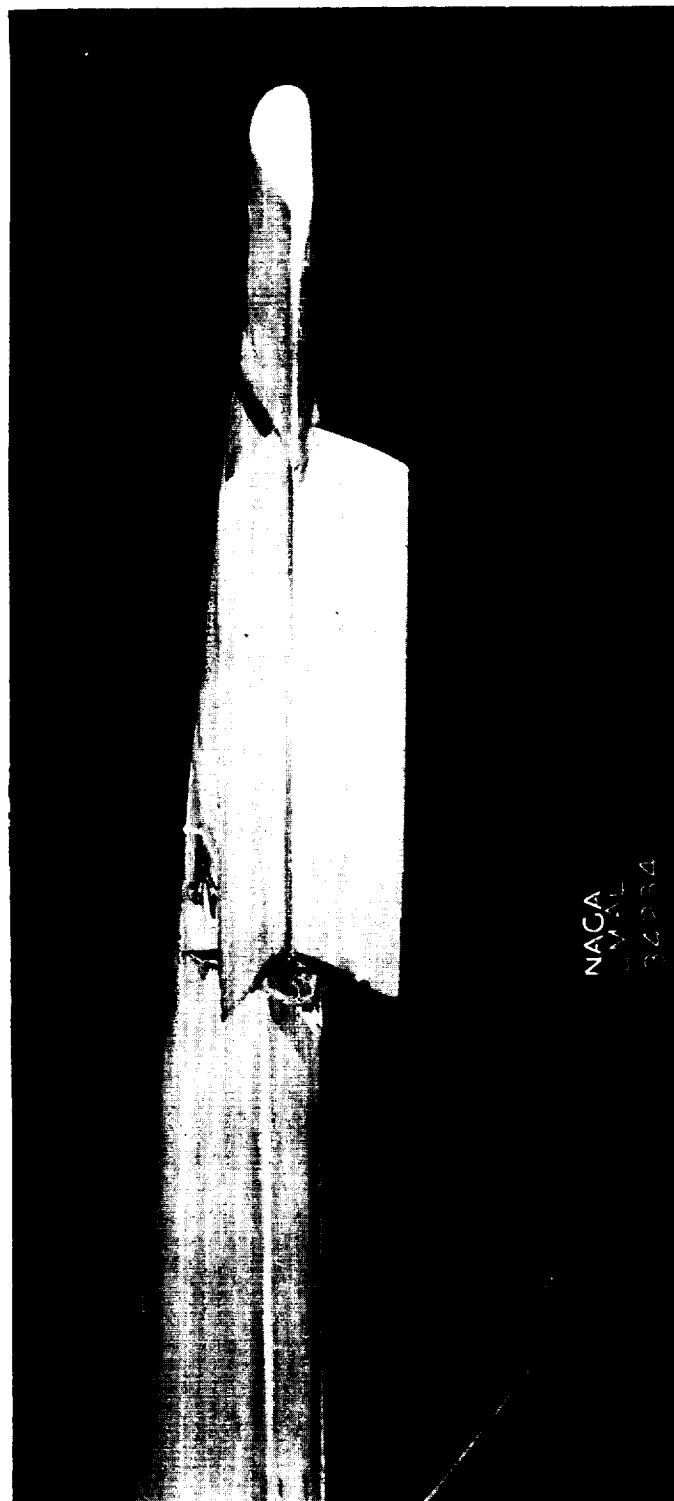
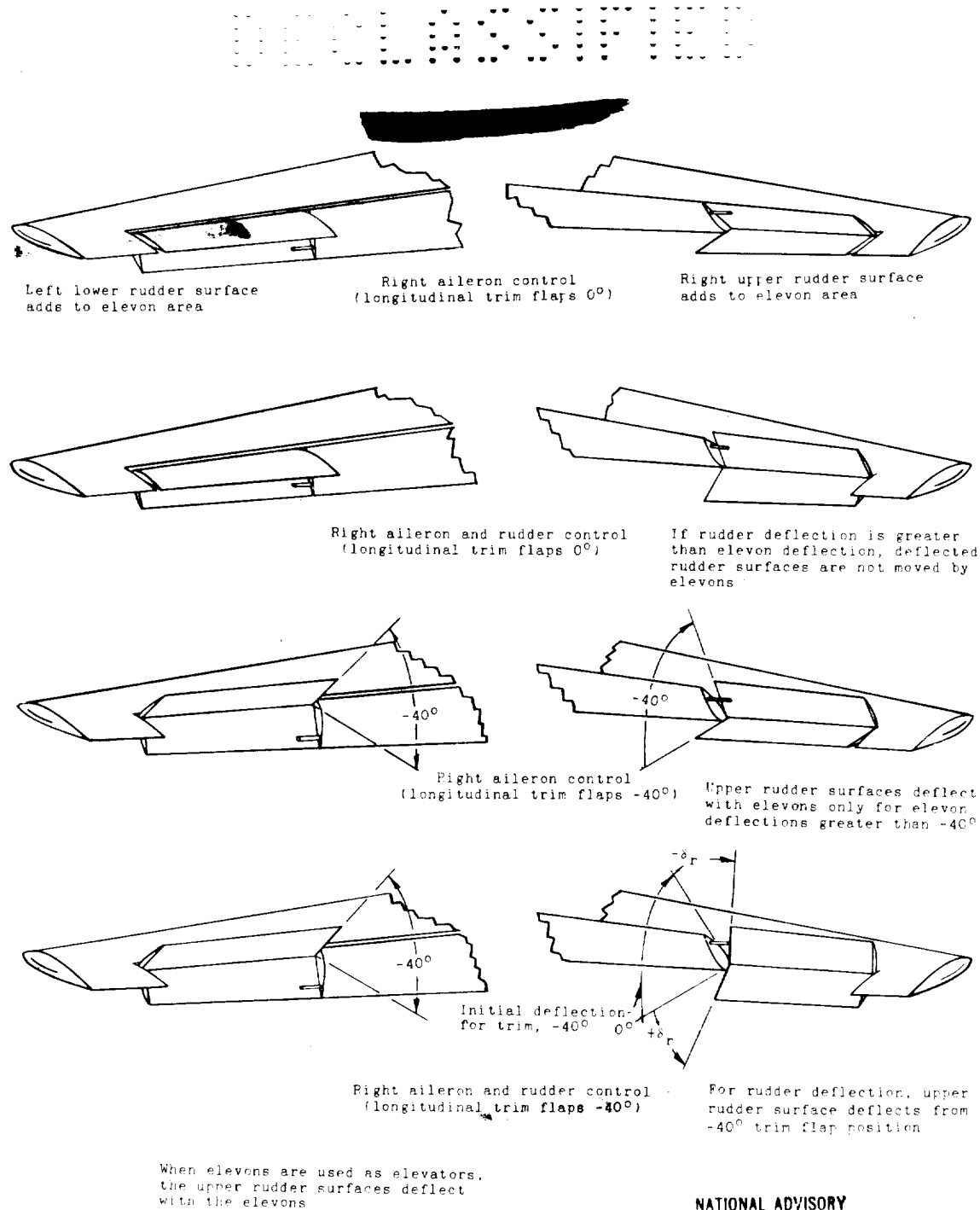


Figure 5.- Split-rudder arrangement used on tailless model tested in Langley free-flight tunnel.

03710001030



NATIONAL ADVISORY  
COMMITTEE FOR AERONAUTICS

Figure 6.- Elevon and rudder arrangement used to obtain additional aileron effectiveness.

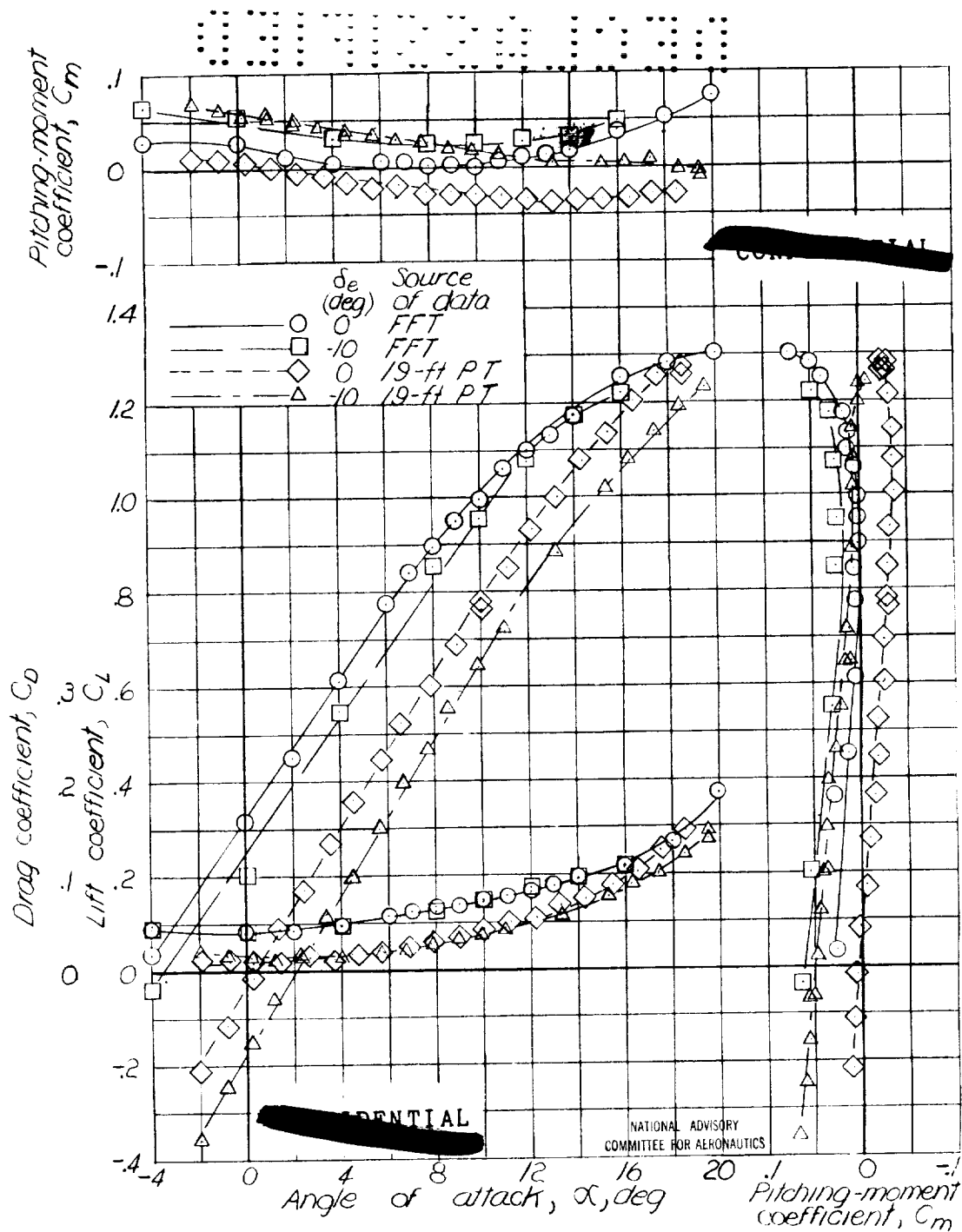


Figure 7.- Lift, drag, and pitching-moment characteristics of models of tailless all-wing airplane with sweepback. Flaps retracted (WHP).



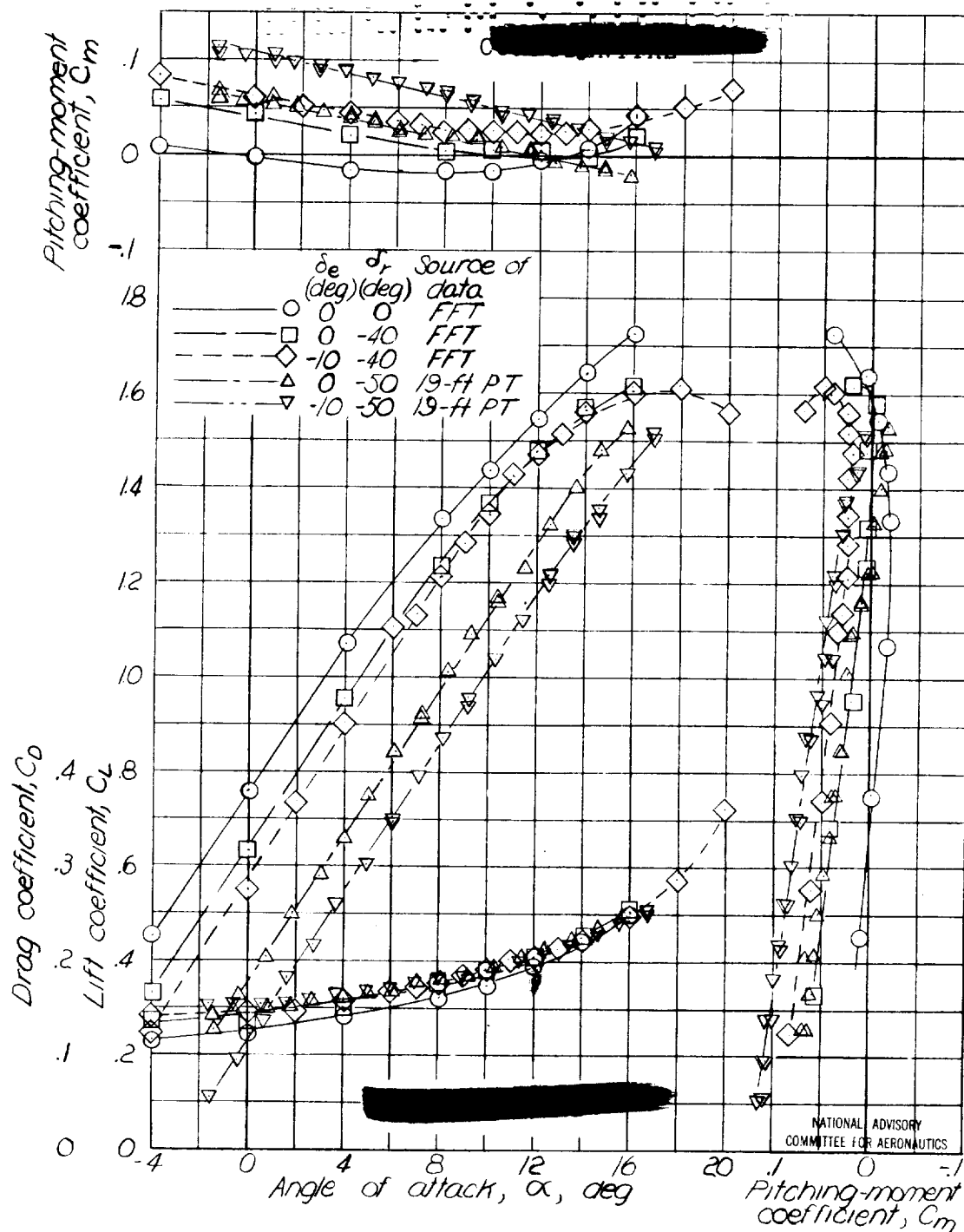


Figure 8.- Lift, drag, and pitching-moment characteristics of models of tailless all-wing airplane with sweepback. Flaps deflected (WHPF).

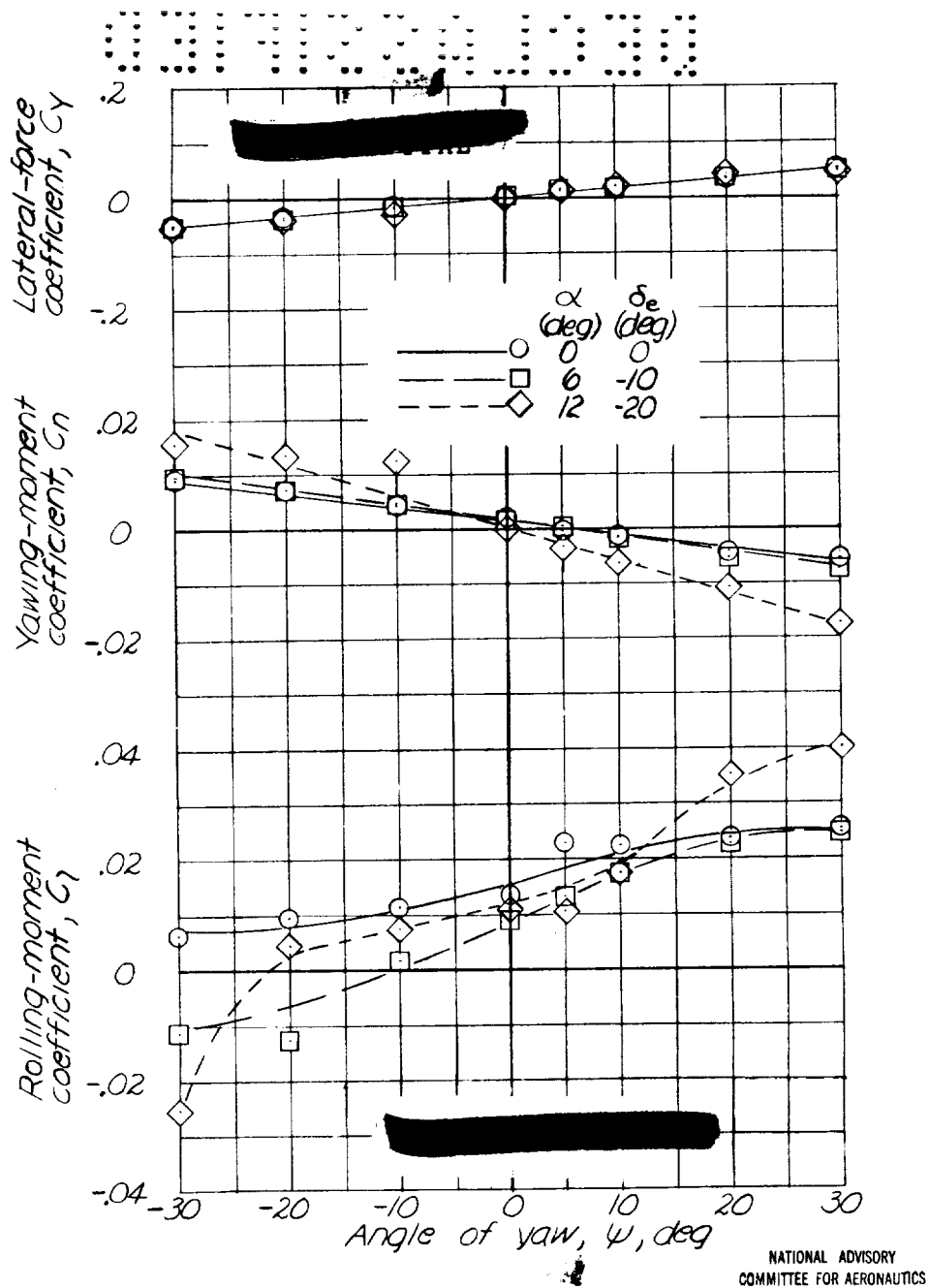
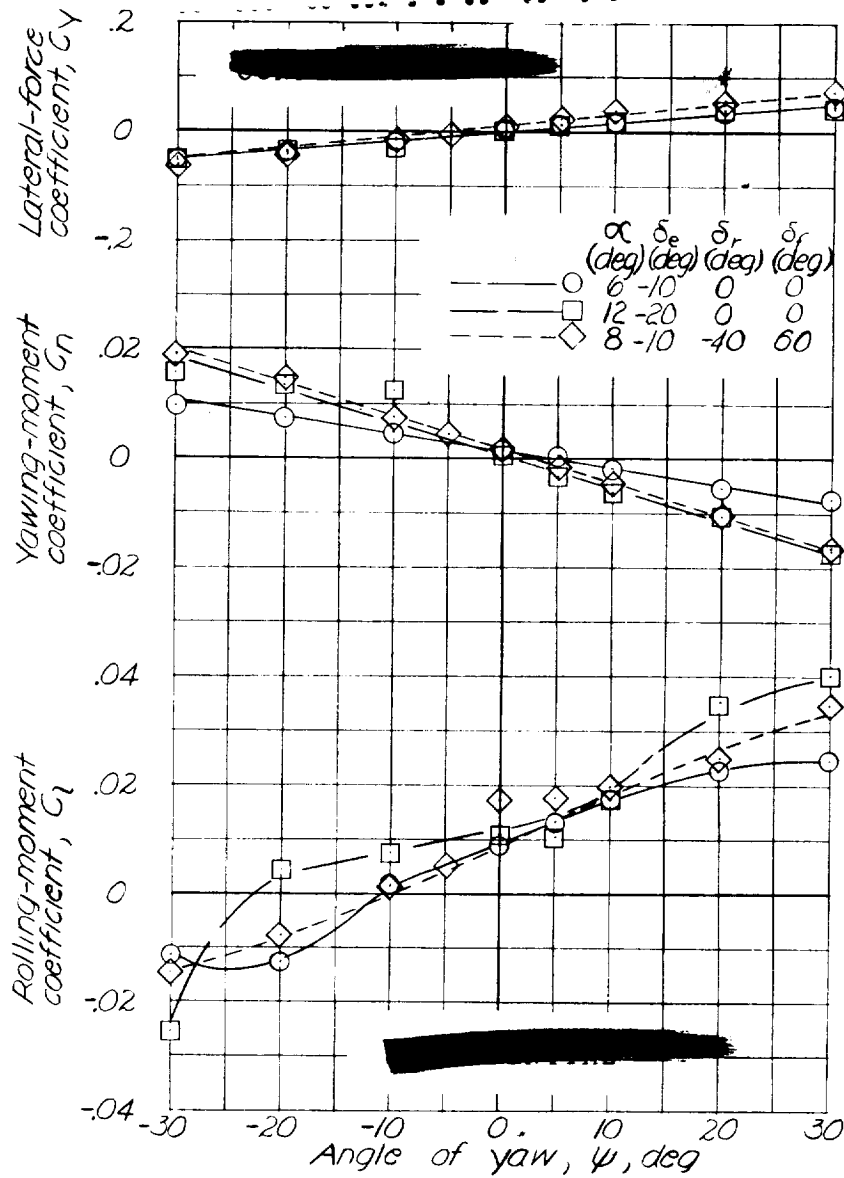


Figure 9.—Effect of angle of attack on the lateral stability characteristics of the Langley free-flight-tunnel model of the tailless all-wing airplane with sweep-back. Flaps retracted (WHP);  $\delta_r = 0^\circ$ .



NATIONAL ADVISORY  
COMMITTEE FOR AERONAUTICS

Figure 10.- Effect of flaps on lateral stability characteristics of Langley free-flight-tunnel model of tailless all-wing airplane with sweepback.

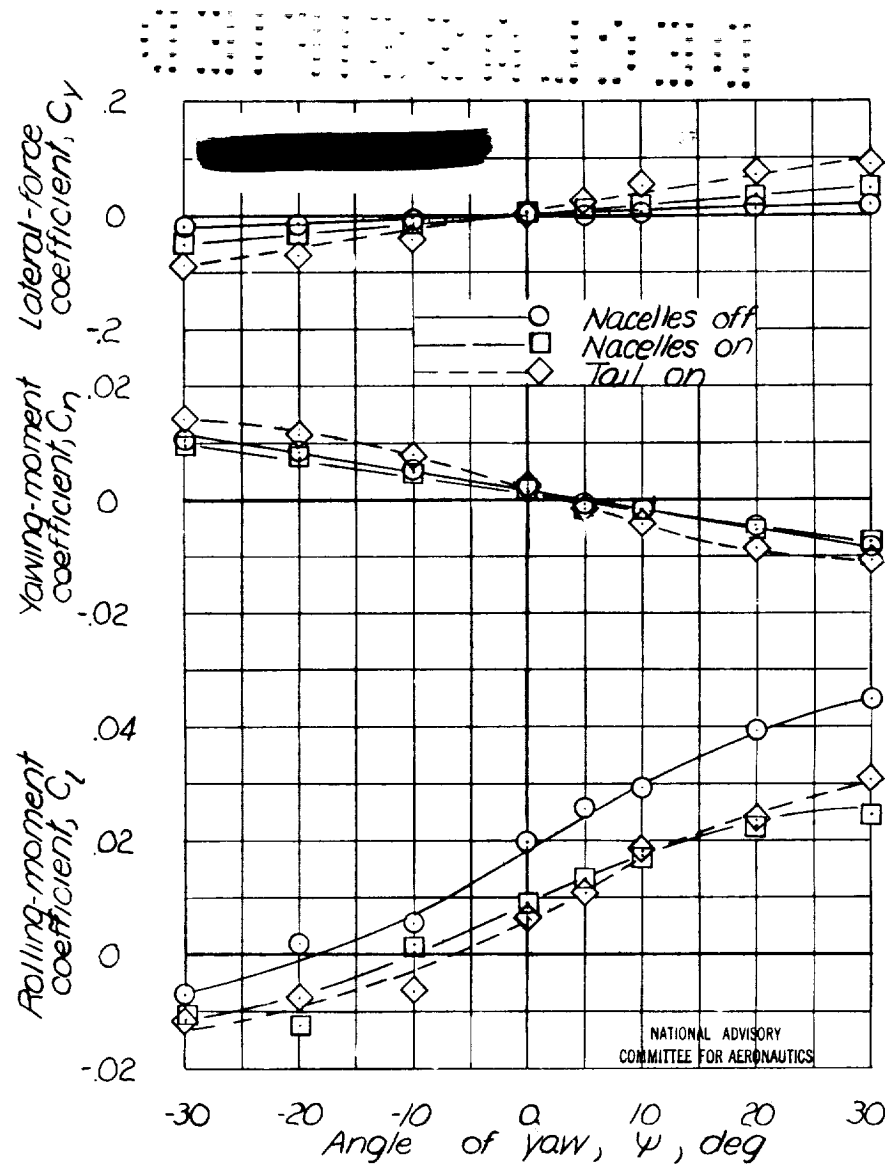


Figure 11.- Effect of propeller housings and vertical tails on lateral stability characteristics of Langley free-flight-tunnel model of tailless all-wing airplane with sweepback.  $\alpha = 6^\circ$ ;  $C_L = 0.70$ .

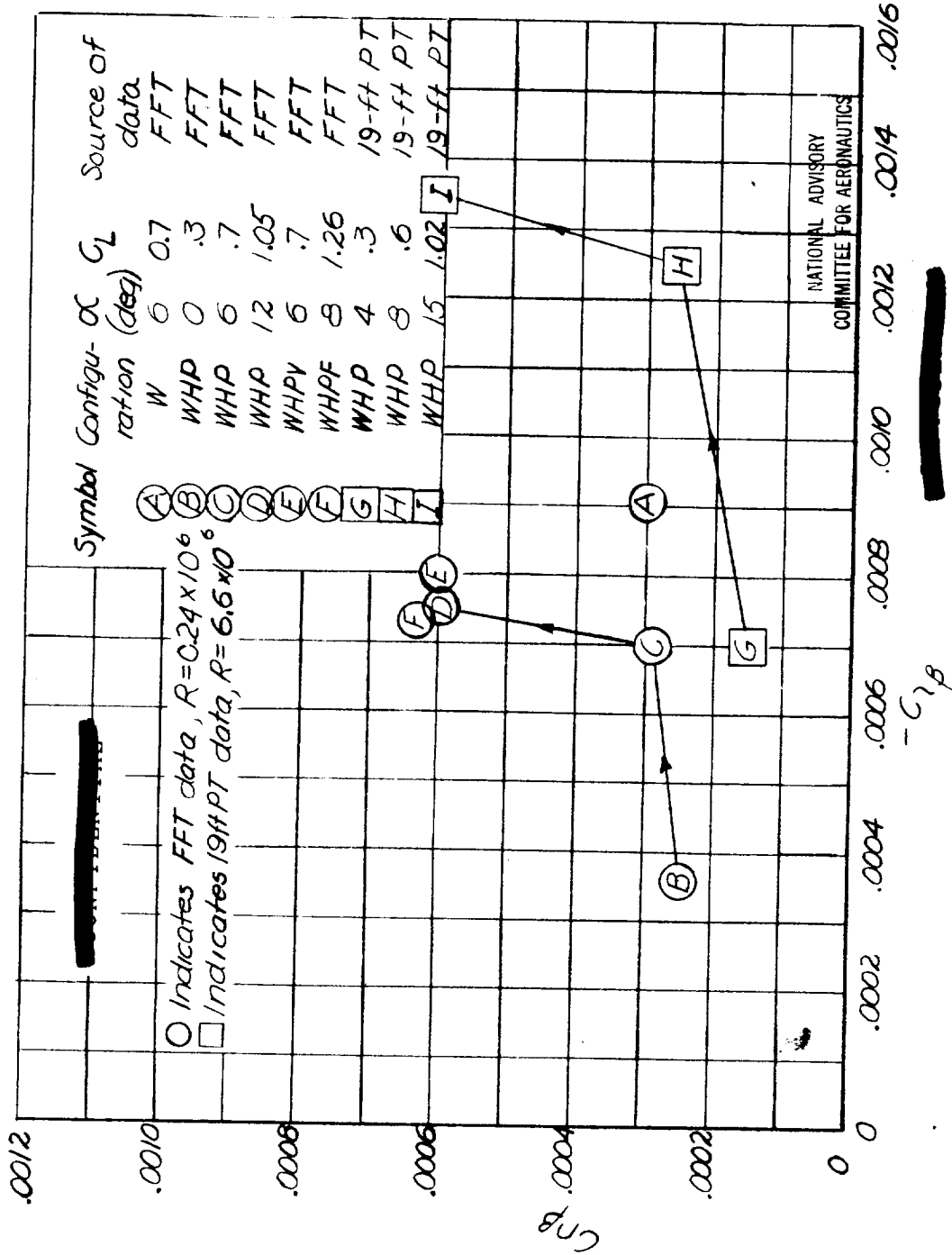
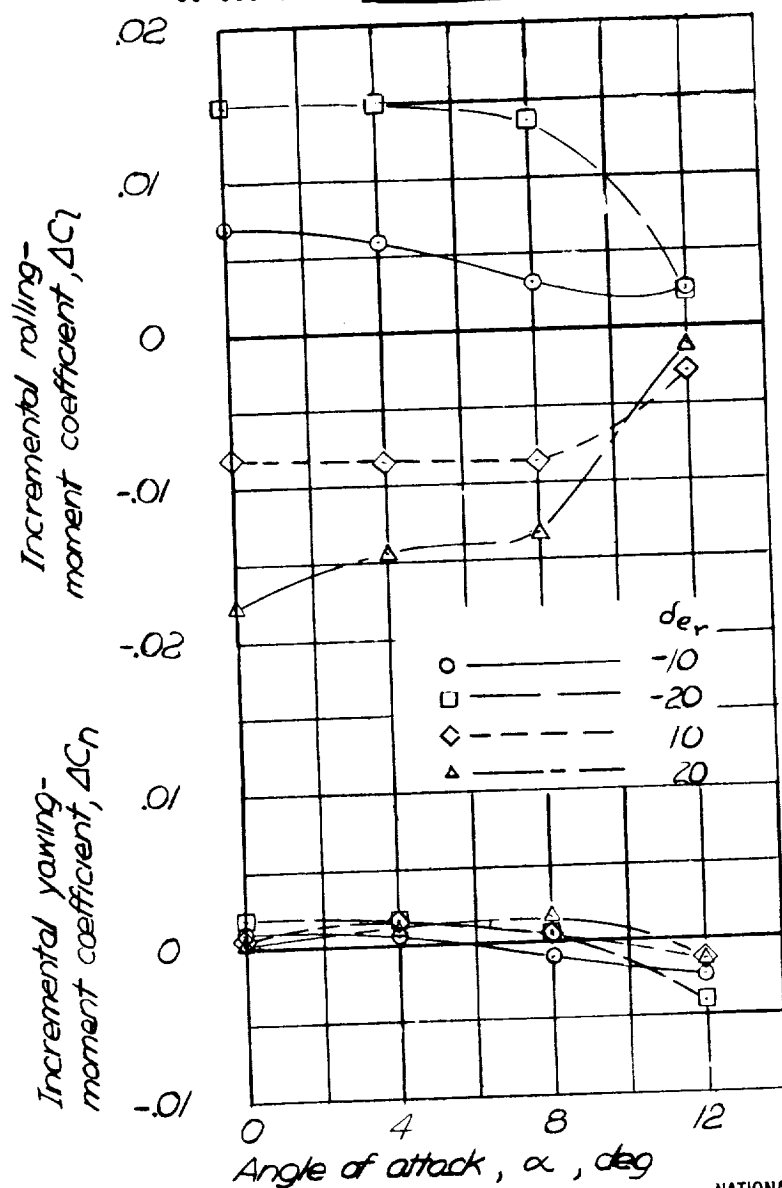
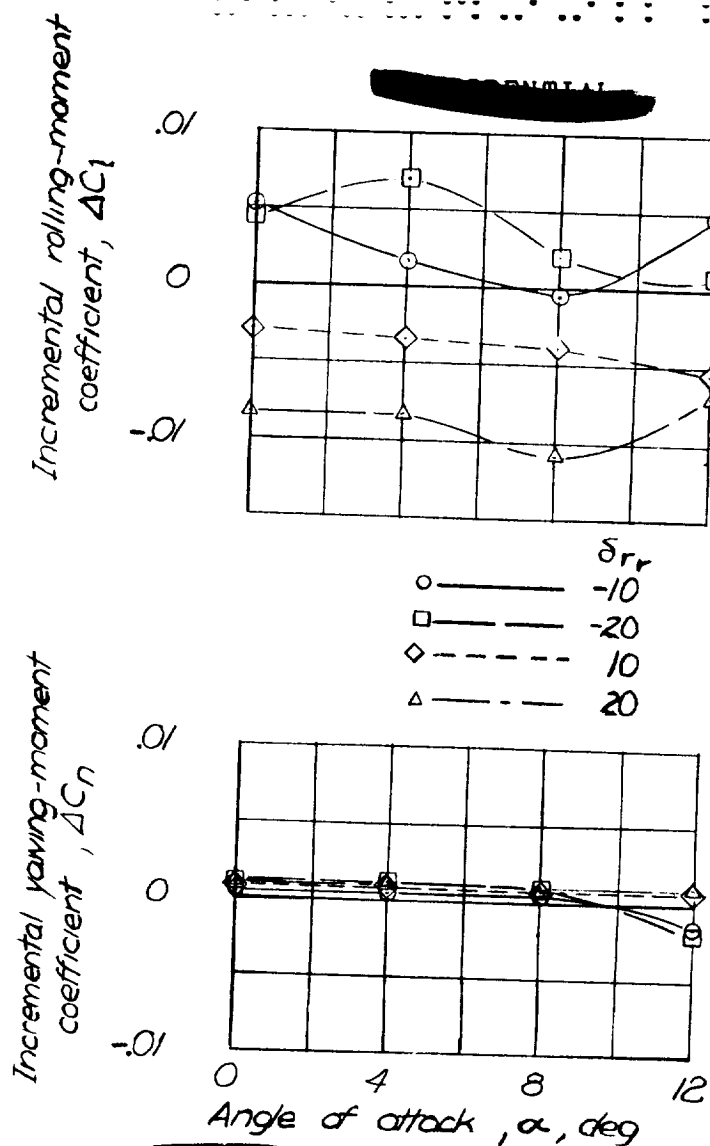


Figure 12.- Values of the lateral-stability parameters  $C_{n\beta}$  and  $C_{\zeta\beta}$  for various configurations of a tailless all-wing airplane as tested in Langley free-flight tunnel and 19-foot pressure tunnel.



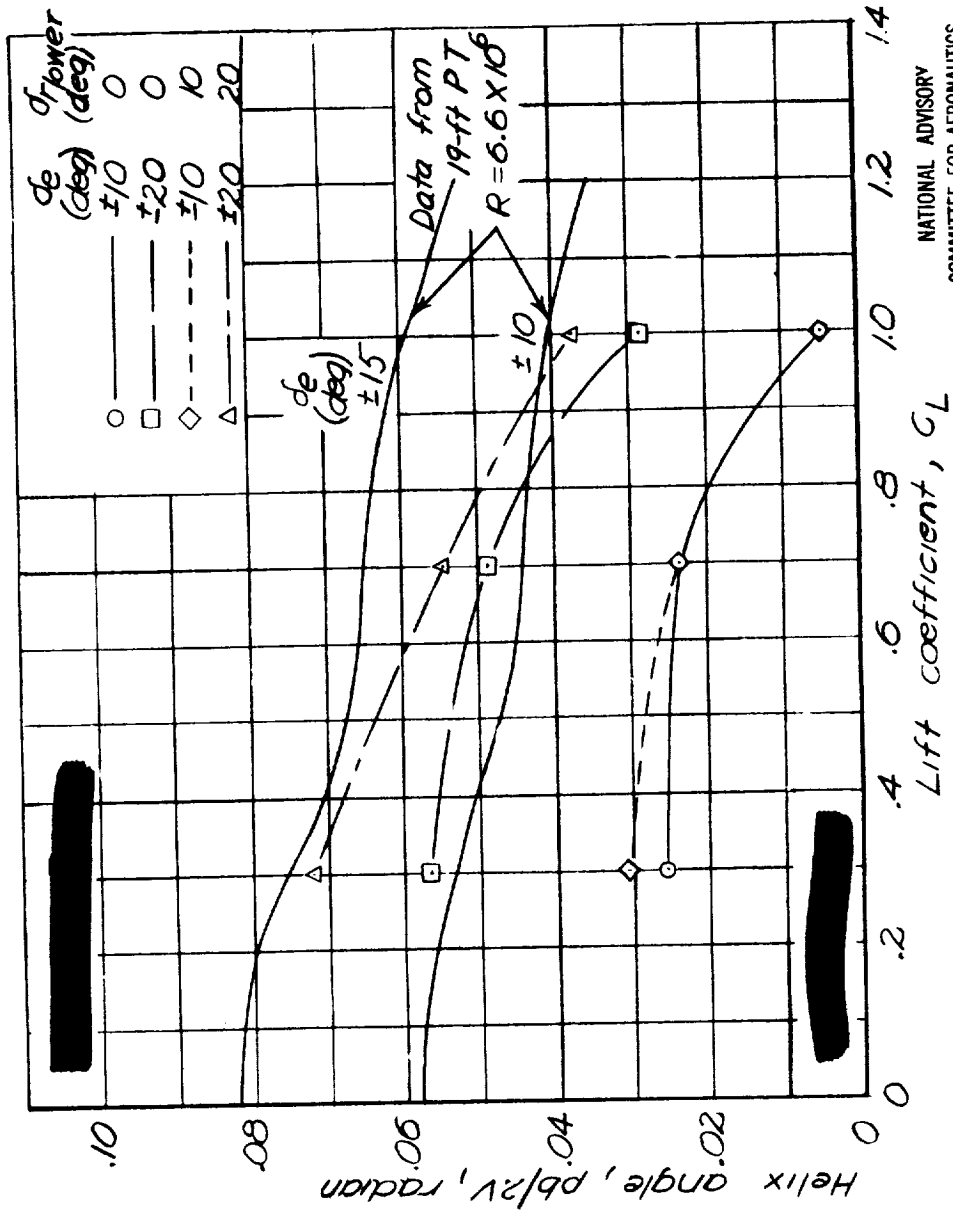
NATIONAL ADVISORY  
COMMITTEE FOR AERONAUTICS

Figure 13.- Variation of elevon effectiveness with angle of attack for Langley free-flight-tunnel model of tailless all-wing airplane with sweepback.



NATIONAL ADVISORY  
COMMITTEE FOR AERONAUTICS

Figure 14.—Rolling and yawing moments produced by deflecting as elevons the split rudders on the Langley free-flight-tunnel model of a tailless all-wing airplane with sweepback.



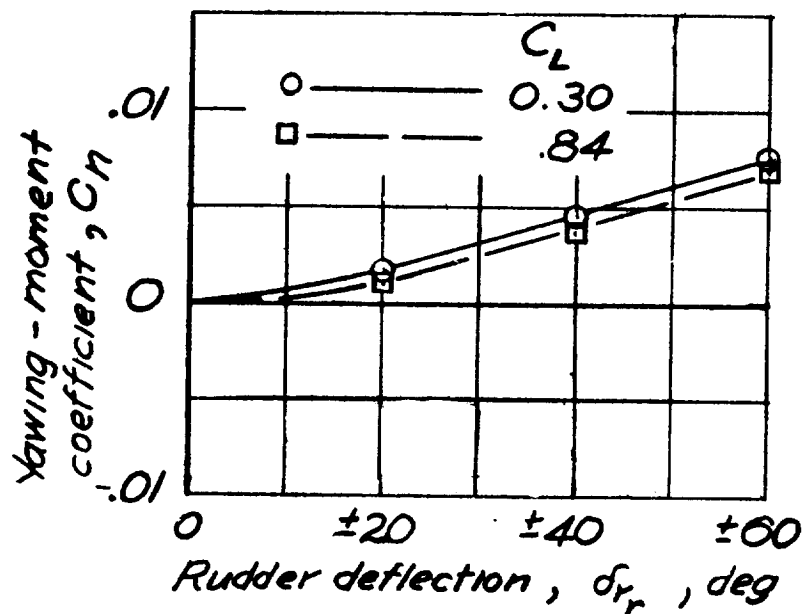
NATIONAL ADVISORY  
COMMITTEE FOR AERONAUTICS

Figure 15.—Variation of aileron effectiveness for equal up and down deflections of elevons from trim position for tailless all-wing airplane model tested in Langley free-flight tunnel.



CONFIDENTIAL

CONFIDENTIAL



NATIONAL ADVISORY  
COMMITTEE FOR AERONAUTICS

Figure 16.- Yawing moments produced by right split-rudder deflection on the Langley free-flight-tunnel model of a tailless all-wing airplane with sweepback.

05712901930

1

2